JOURNAL OF MATERIALS SCIENCE 8 (1973) 851–858

Formation of metastable phases in flame- and plasma-prepared alumina

R. McPHERSON
Department of Materials Engineering, Monash University, Clayton, Victoria, Australia, and Division of Inorganic and Metallic Structure, National Physical Laboratory, Teddington, UK

The formation of metastable phases in plasma- and flame-prepared alumina particles is examined in terms of the classical nucleation theory, rate of transformation of metastable to stable forms, and the thermal history of the particles during solidification. It is suggested that homogeneous nucleation of the solidification of liquid droplets at considerable undercooling results in the formation of γ-Al_2O_3 rather than α-Al_2O_3 because of its lower critical free energy for nucleation. The phase finally observed depends upon the thermal history of the particles during evolution of the heat of fusion and upon the kinetics of the transformation of the nucleating phase to the stable phase. This means that the cooling rate of the particles is relatively unimportant and under the conditions existing in flames and plasmas, metastable alumina will be formed on solidification. The metastable form will be retained on cooling particles less than approximately 10 μm diameter, but particles larger than this may transform to α-Al_2O_3 during the solidification exotherm

1. Introduction

Spherical particles of alumina prepared by flame [1] and plasma [2] melting of powders, by condensation of vapour from arcs [3] and high-frequency plasma [4] or flame [5] oxidation of aluminium chloride, have been reported to consist predominantly of metastable phases (γ-Al_2O_3, δ-Al_2O_3 and θ-Al_2O_3) rather than the stable α-Al_2O_3 form. Plasma-sprayed coatings also consist of metastable forms [6, 7] although if deposited onto a heated substrate, some α-Al_2O_3 is produced [8].

Plummer [1] observed that α-Al_2O_3 tended to be produced in flame spheroidized particles larger than approximately 15 μm diameter and he suggested that metastable phases were formed at fine particle sizes because their more rapid cooling rate resulted in "quenching in" of the assumed tetrahedral co-ordination of aluminium by oxygen in the liquid state. This would then tend to produce solid phases with cubic close packing of oxygen ions (γ-, δ-, θ-Al_2O_3) rather than the hexagonal packing of α-Al_2O_3. Das and Fulrath [2] also observed that although a metastable form (γ-Al_2O_3) predominated in particles less than 10 μm diameter spheroidized in a d.c. plasma jet, α-Al_2O_3 was formed at larger particle sizes, and the ratio of γ-Al_2O_3 to α-Al_2O_3 could be related to a quenching parameter. They suggested that the rates of nucleation of the two phases from the liquid determined the proportions observed in the product, however they did not take into account the possible transformation of γ-Al_2O_3 to α-Al_2O_3 which may occur at temperatures greater than approximately 1200° C. A similar dependence of structure on particle diameter has also been observed in micron-sized alumina particles prepared by treatment of submicron powders in a flame reactor [9].

In this paper it is suggested that homogeneous nucleation of solidification of liquid droplets at considerable undercooling, results in the formation of γ-Al_2O_3 rather than α-Al_2O_3 because of its lower critical free energy for nucleation. The phase finally observed depends upon the thermal history of the particles during the evolution of the heat of fusion, and the kinetics of the transformation of γ-Al_2O_3 to α-Al_2O_3.

2. Nucleation from the vapour

Spheroidization of micron-sized solid particles is clearly a melting operation, however the question arises whether submicron particles prepared by flame or plasma oxidation of aluminium halides,

condense as liquid droplets which subsequently freeze, or by direct condensation to solid.

The partial pressure of aluminium oxides in equilibrium with liquid Al_2O_3 at T_m and an oxygen pressure of 1 atm is of the order of 10^{-9}, calculated from JANAF thermodynamic data [10]. Nucleation and growth of Al_2O_3 from the vapour must therefore occur as the liquid phase for plasma and flame conditions in which gas temperatures are considerably greater than T_m and initial oxide partial pressures are many orders of magnitude greater than 10^{-9}.

The fact that flame and plasma prepared Al_2O_3 particles are spherical is consistent with condensation as droplets followed by solidification, since the growth of solid from the vapour would be expected to lead to the formation of particles with crystalline facets because of the elimination of high-index planes during growth [11]. This is supported by the observations that particles of Cr_2O_3 condensed from a plasma [4] and MgO condensed from an arc [12] occur with crystalline facets, since the vapour pressures of these oxides are relatively high at T_m (or more correctly at the solidification temperature $T_S \simeq 0.8\ T_m$, see below).

3. Solidification of isolated droplets

It is well established that solidification of most of the particles in a collection of isolated droplets is initiated by homogeneous nucleation and occurs at a temperature considerably below the equilibrium melting point. Generally only a small proportion of the droplets, which it is assumed contain pre-existing nuclei, solidify at a temperature close to T_m.

The rate of nucleation is given by the classical steady-state equation

$$I = \mathrm{A} \exp(-\Delta G^*/kT) \qquad (1)$$

where A may be regarded as a constant because of the preponderance of the exponential term

$$\Delta G^* = 16\pi\gamma^3/3\Delta G_v^2 . \qquad (2)$$

For solidification ΔG^* may be written [13]:

$$\Delta G^* = K\gamma^3 T_m^2/\Delta H_v^2 \Delta T^2 , \qquad (3)$$

where I = nucleation rate per unit volume, ΔG^* = critical free energy for nucleation, k = Boltzmann's constant, γ = interfacial surface energy, ΔG_v = free-energy change per unit volume of product, K = nucleus shape factor, ΔH_v = heat of fusion per unit volume of crystal and ΔT = undercooling.

There is considerable uncertainty in the pre-exponential term of the nucleation equation (the experimental value [14] is of the order of 10^{42} cm^{-3} sec^{-1}); however, this is relatively unimportant compared with the large changes in the exponential term produced by small temperature changes.

The freezing of a droplet is a statistical process depending upon the chance formation of a nucleus, and the probability of freezing will therefore depend upon the volume of the drop and the cooling rate [15]. Since the nucleation rate increases extremely rapidly with decreasing temperature, the range of solidification temperature of a group of particles will be quite small.

Experimentally it has been found that the solidification temperature of a group of isolated particles is 0.82 T_m for a wide range of metals [16] and ionic solids [17], in the particle size range 10 to 1000 μm and at slow cooling rates. For plasma- and flame-prepared particles the cooling rates are high (10^3 to 10^6 °C sec^{-1}) so that solidification temperatures lower than 0.82 T_m would be expected. Values of T_S for Al_2O_3 given in Table I were calculated from Equations 1 and 3 for a cooling rate of 10^4 °C sec^{-1} and assuming that $T_S = 0.82\ T_m$ for particles of diameter $d = 50\mu$m, at a cooling rate of 10^{-2} °C sec^{-1} and that the nucleation rate per particle is 10^{-1} sec^{-1} under these conditions [13]. The pre-exponential factor, A, was taken as 10^{42} cm^{-3} sec^{-1}.

Turnbull [14] has pointed out that the crystal nucleus may not be the phase with the lowest free energy but an alternative structure which has a lower ΔG^*. This effect was later observed experimentally by Cech [18] who found that isolated droplets of an Fe-Ni alloy solidified as the bcc structure (α) rather than the equilibrium fcc structure (γ). Small particles, which had a slow cooling rate in the apparatus used, tended to transform from α to γ after solidification.

A similar phenomenon could account for the formation of metastable forms in alumina particles prepared by high-temperature techniques. If the initial nucleus is not the equi-

TABLE I Estimated solidification temperatures (T_S) of Al_2O_3 as a function of particle diameter for a cooling rate of 10^4 °C sec^{-1}

d (μm)	T_S (°C)
100	1585
10	1570
1	1550
0.1	1500

librium structure, a metastable phase will be observed at room temperature if the rate of crystal growth from the liquid is faster than the rate of transformation to the stable phase, and the cooling rate after solidification is sufficiently rapid to suppress subsequent transformation. The phase which is finally observed will therefore depend upon the relative critical free energies of nucleation of alternative crystal structures, the kinetics of the transformation from non-equilibrium to equilibrium forms and the thermal history of the particles.

In view of the rapid cooling rate of particles in plasmas and flames, nucleation of solid from liquid droplets could be a transient rather than steady-state problem. The delay time for the establishment of an equilibrium distribution of embryos has been treated by Buckle [19] for the initial conditions of zero embryo concentration and for an initial Maxwell-Boltzmann distribution. However, Courtney [20] has shown that the latter assumption is the more realistic approach and using appropriate values for Al_2O_3, the estimated time lag is of the order of 10^{-6} sec; the steady-state equation should therefore be applicable.

The relative nucleation rates of two alternative structures will depend upon the ratio of the critical nucleation free energies, $\Delta G_1^*/\Delta G_2^*$, which in principle may be estimated from Equation 2. Practical application of the nucleation equation is limited, however, because of the sensitive dependence of ΔG^* on the liquid-solid interfacial energy, values for which are not generally available. Turnbull [16] observed that there is a relationship between the surface energy per mole (γ_g) and the heat of fusion per mole (ΔH_m).

$$\gamma_g = k\,\Delta H_m \qquad (4)$$

$$\gamma_g = N^{1/3} V_m^{2/3} \gamma \qquad (5)$$

where N = Avogadro Number and V_m = molar volume. The factor k is found to lie between 0.3 and 0.6 and depends upon the type of crystal structure. Since k could differ for two different forms of the same substance, an alternative approach for the estimation of γ due to Skapski [21] has been used. On the basis of a next-neighbours analysis he obtained (neglecting a third entropy term which is relatively unimportant):

$$\gamma = (Z_i - Z_a)\,\Delta H_m / Z_i N^{1/3} v_m^{2/3} + 2\Delta V \gamma_L / 3V_g \qquad (6)$$

where Z_i = number of next-neighbours surrounding an atom in the interior of the solid or liquid phase, Z_a = number of neighbours of an atom at the surface of the solid, $\Delta V/V_s$ = fractional volume change on melting, and γ_L = liquid surface tension.

Values of liquid-solid interfacial energy determined for a number of metals using this equation have given good agreement with values determined from nucleation experiments by Turnbull.

The interfacial energies for α-Al_2O_3 and γ-Al_2O_3 have been estimated using Equation 6 and the following data:

$$\frac{Z_i - Z_a}{Z_i} = \tfrac{1}{4}$$

ΔH_m (α-Al_2O_3) = 21.4 kcal mol^{-1} [22]

ΔH_m (γ-Al_2O_3) = 16 kcal mol^{-1},

estimated from the heat of fusion of α-Al_2O_3, the heat of transition γ-Al_2O_3 to α-Al_2O_3 [23], and the enthalpies of α-Al_2O_3 and γ-Al_2O_3[10]. Densities of α-Al_2O_3 and γ-Al_2O_3, 4.0 and 3.4 g cm^{-3} [24].

Volume change on melting of α-Al_2O_3 = 20% [25].

Surface tension of liquid Al_2O_3 at T_m = 690 dyne cm^{-1} [25].

The resulting values for the liquid-solid interfacial energy are

γ-Al_2O_3 240 erg cm^{-2}

α-Al_2O_3 390 erg cm^{-2}.

The difference in free energy between solid and liquid as a function of temperature for α-Al_2O_3 and γ-Al_2O_3 was determined from JANAF data [10], and the ratio of $\Delta G_\alpha^*/\Delta G_\gamma^*$ based on these results is shown in Fig. 1 as a function of temperature. On this basis γ-Al_2O_3 would be nucleated rather than α-Al_2O_3 at temperature

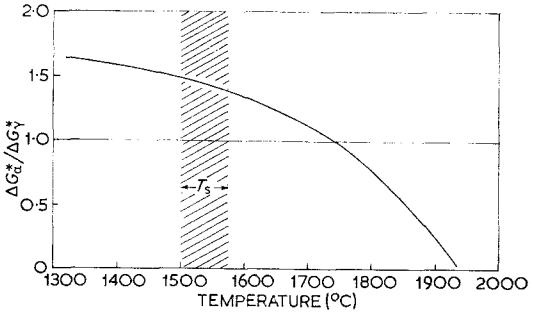

Figure 1 Estimated ratio of critical free energies for nucleation of alpha and gamma alumina as a function of temperature.

less than 1740°C. Comparison with the estimated solidification temperatures given in Table I suggests that nucleation of γ-Al_2O_3 will occur in isolated droplets of alumina; the nucleation rate of α-Al_2O_3 will be orders of magnitude smaller and may be regarded as negligible.

4. Particle temperatures in plasmas and flames

Because of the high heat-transfer rates between small particles and their surrounding gas (see below), liquid droplets dispersed in flame or plasma exhaust gases would be expected to be close to thermal eqilibrium with the gas, and the cooling rate of the particles will be determined predominantly by the gas cooling rate. Gas temperatures as a function of distance from the work coil in the confined tail flame of an oxygen–argon r.f. plasma have been determined by Bayliss [26], and indicate a cooling rate of the order of 10^3 deg sec^{-1} at 2000 K. This value may be regarded as a lower limit; faster rates would be expected for plasmas containing dispersed particles because of heat loss from the system by radiation from the particles, or for plasmas in which mixing with cool gas occurred. Measurements of gas temperature in an argon d.c. plasma jet indicate cooling rates of the order of 10^6 deg sec^{-1} at 3000 K [27], and similar cooling rates are suggested from the calculated temperatures of dispersed particles in a plasma jet confined within a water-cooled channel [28].

Dispersed liquid droplets will cool in the tail flame from a plasma or flame until nucleation occurs at T_s, followed by rapid initial crystallization since no heat transfer is necessary to form solid at T_m from super-cooled liquid. Liberation of the heat of fusion will increase the liquid temperature and suppress further nucleation so that, in general, solidification would be expected to occur as a single crystal from the first nucleus to form.

Below T_m the rate of solidification, and hence the rate of heat evolution, will be limited by the rate of transfer of atoms from liquid to crystal at the growing interface. The mean particle temperature will therefore depend upon the limiting growth velocity and the heat-transfer coefficient between particle and gas. If $\Delta H_m > C_p \Delta T$ (C_p = heat capacity) the particle temperature may increase to T_m, the rate of solidification then being controlled by the rate of heat loss and the particle temperature would remain at T_m until solidification was complete. The temperature-time profile during solidification of a droplet may therefore be calculated by conventional heat-transfer methods if the rate of initial crystallization is known.

Data on the limiting growth velocity of crystals is not generally available, however the order of magnitude may be estimated using the analysis of Cahn *et al* [29] for the continuous growth velocity (Γ) of a crystal at large undercooling.

$$\Gamma = \beta D \Delta H_m \Delta T / aRT^2 \qquad (7)$$

where β = kinetic correction factor $\simeq$ 10 in this case, D = liquid self diffusion coefficient, a = growth step height, and R = gas constant. The use of McKenzie's data [30] for the viscosity of liquid Al_2O_3 and assuming that a is equal to the lattice parameter of γ-Al_2O_3 gives a growth velocity of the order of 10 cm sec^{-1} in the range ΔT = 50 to 500 K.

For small spherical particles with low velocity relative to the gas (Reynolds No. < 1), the convective heat-transfer coefficient (h) is [31] $h = 2k_g/d$, where k_g = thermal conductivity of the gas and d = particle diameter.

The simplifying assumption may also be made of infinite thermal conductivity of the particle, justified if the Biot Number (Bi) is small (Bi = $hd/2k_p$ where k_p = thermal conductivity of the particle). For particles of Al_2O_3 smaller than 50 μm diameter Bi < 10^{-2}. The convective heat-transfer coefficient is much greater than the radiative heat-transfer coefficient for the conditions examined here and heat loss from the particles by radiation has therefore been neglected.

Assuming linear release of the heat of fusion with time until solidification is complete (for γ-Al_2O_3, $\Delta H_m \simeq C_p \Delta T$, and there will be no thermal arrest at T_m) the particle temperature as a function of time (θ) from nucleation is given by

$$1 - 3h(T - T_g)/\rho\Gamma\Delta H_m = \exp(-6h\theta/\rho C_p d) . \qquad (8)$$

The cooling rate after solidification is given by [31]

$$T - T_g/T_{max} - T_g = \exp(-6h\theta'/\rho C_p d) \qquad (9)$$

where ρ = particle density, C_p = heat capacity, T_g = gas temperature, T_{max} = maximum particle temperature, θ = time from nucleation until complete solidification and θ' = time from solidification ($\theta' = 0$ when solidification is complete). These calculations assume constant gas temperature which is satisfactory for cooling rates up to approximately 10^4 °C sec^{-1}.

Fig. 2 shows the calculated temperature-time

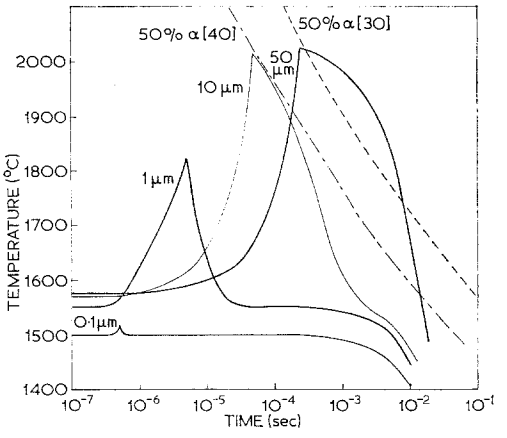

Figure 2 Calculated thermal history of alumina particles in an oxygen stream cooling at 10^4 °C sec^{-1}. Extrapolated 50% transformation of γ-Al_2O_3 to α-Al_2O_3 data in the presence of [40] and absence of [38] water vapour is also shown.

curves for the solidification of alumina droplets assuming a gas cooling rate of 10^4 deg sec^{-1} and gas thermal conductivity of 2.4×10^{-4} cal sec^{-1} cm^{-1} $°C^{-1}$ (oxygen at 1500 K) [32].

5. Transformation to the equilibrium structure

A number of metastable forms of Al_2O_3 have been reported and of these the γ, δ and θ-modifications have been detected in flame- and plasma-prepared materials. Studies of the dehydration of boehmite [33] and the transformation of vapour-deposited amorphous alumina to α-Al_2O_3 [34] indicate that γ-Al_2O_3 and δ-Al_2O_3 are the principal intermediate forms before the formation of α-Al_2O_2 with θ-Al_2O, as a minor constituent. Although the details of the crystal structures of the metastable forms are not completely clear, it is apparent that γ, δ and θ-Al_2O_3 are based on a more or less distorted cubic close packing of oxygen ions with different ordering of the Al ions in the available octahedral and tetrahedral sites [33, 35]. Gamma alumina has a spinel structure in which all of the octahedral sites are occupied and the tetrahedral lattice has vacant sites. The δ-Al_2O_3 form has a well-ordered superspinel structure although some disorder persists in the direction of the *c*-axis [33].

The kinetics of the transformation of submicron γ-Al_2O_3 to α-Al_2O_3 has been studied by Steiner *et al* [36]. The presence of water vapour has been reported to increase the transformation rate of γ-Al_2O_3 [37], and kinetic data for the transformation in the presence of water has been published [38]. Rate constants for both sets of data were extrapolated to higher temperatures and the times for 50% transformation have been plotted in Fig. 2. The percentage transformation of γ-Al_2O_3 to α-Al_2O_3 was calculated by a stepwise method at 50° intervals for particles of various diameters using the temperature time data of Fig. 2 and Steiner *et al* kinetic data to produce the results shown in Table II.

These results show that spheroidized powders consisting of particles larger than 10 μm would be expected to contain some α-Al_2O_3, and that particles larger than 50 μm would consist entirely of α-Al_2O_3. Since water vapour increases the transformation rate, the particle sizes at which α-Al_2O_3 is observed may be somewhat smaller for flame prepared powders.

This analysis may be compared with experimental observations of the structure of flame spheroidized [1, 5, 9] and plasma spheroidized [2] alumina particles. Plummer [1] observed that α-Al_2O_3 did not occur in particles smaller than 15 μm and that metastable forms did not occur in particles larger than 35 μm diameter. He also noted that changes in flame temperature had little influence on the constitution of the particles. Cuer *et al* [5, 9] observed that spherical particles with diameters in the range 120 to 1200Å prepared by flame oxidation of $AlCl_3$ consisted of δ-Al_2O_3 whereas particles with a mean diameter of 4.7 μm prepared by passing submicron powder through a flame reactor consisted of δ-Al_2O_3 and θ-Al_2O_3. A mixture of δ, θ- and α-Al_2O_3 was observed in particles with a mean diameter of 47 μm and the proportion of α-Al_2O_3 could be increased by passing the flame tail gas through a heated tube at 1001 to 1500°C.

Das and Fulrath [2] observed a considerable density range in alumina particles spheroidized by means of an argon-hydrogen d.c. plasma jet, many of the particles in the diameter range 50 to 175 μm consisting of hollow spheres. For air elutriated particle fractions of near theoretical

TABLE II Percentage transformation to α-Al_2O_3 as a function of particle diameter

Diameter (μm)	% α-Al_2O_3
1	0
10	9
20	40
50	100

density the observed ratios of metastable to stable phase (R) were: particle diameter 7 to 14 μm, $R = 40$ to 100; particle diameter 53 to 61 μm, $R = 2 \times 10^{-3}$. For a given particle size range the value of R varied with apparent density, for example in the diameter range 61 to 74 μm the value of R ranged from 10^3 at 30% theoretical density to 0.1 at approximately 80% theoretical density. They also observed that γ-Al_2O_3 was the predominant metastable phase in small particles but the proportion of δ-Al_2O_3 increased with increasing diameter.

The calculated particle diameters of 10 μm at which α-Al_2O_3 is first observed and 50 μm at which α-Al_2O_3 is the predominant phase is therefore in good agreement with the experimental data. The effect of porosity on the structure finally observed [2] is consistent with the hypothesis that α-Al_2O_3 is formed by transformation of γ-Al_2O_3 during the solidification exotherm since a hollow spherical shell would be equivalent to a smaller solid particle.

Sprayed alumina coatings are formed by the solidification of liquid droplets which flatten as they strike the surface [6]. The particles are therefore rapidly quenched when sprayed onto a cool substrate and the transformation to α-Al_2O_3 is suppressed. Alpha alumina may be formed if the cooling rate is reduced by spraying onto a heated substrate; however, a substrate temperature of 1450°C is required for the preparation of completely α-Al_2O_3 coatings [8].

Kinetic data for the γ-Al_2O_3 to δ-Al_2O_3 transformation are not available, however the transition to δ-Al_2O_3 would be expected to nucleate more easily than that to α-Al_2O_3 since it does not require rearrangement of the oxygen ions. Dragoo and Diamond [34] suggest that δ-Al_2O_3 is formed from γ-Al_2O_3 in the temperature range 800 to 1200°C. Evidence for the nucleation of γ-Al_2O_3 rather than other metastable forms is provided by the observation of γ-Al_2O_3 in sprayed coatings [6, 7] and small particles prepared by d.c. plasma spraying into air [2] in which the rapid cooling rate after solidification could be expected to suppress the γ-Al_2O_3 to δ-Al_2O_3 transformation. Delta-alumina is observed in powders prepared by flame [1, 5] and r.f. plasma [4] methods in which the cooling rate after solidification is considerably lower.

6. Discussion

When a number of alternative crystalline forms of a substance are possible the question arises which of these will be obtained under particular conditions of formation. Ostwald [39], in his empirical law of successive stages, suggested that in all reactions the most stable state is reached by steps from the least stable state, however there are a number of exceptions to the law and Tammann [40] pointed out that the most important factor in crystallization is the comparative rates of nucleation of alternative phases. The classical nucleation theory may be criticized on the grounds that the free energy of nucleus formation is derived from macroscopic quantities, and in particular the macroscopic interfacial energy is used for nuclei which consists of only a few hundred atoms. However, there appears to be no completely satisfactory alternative at the present time and in the case considered here it is the relative free energies of nucleation of alternative structures which are important rather than absolute values of nucleation rate.

Although a number of assumptions have been made and the results of the calculation of nucleation energy barriers must be regarded as approximate, the available data suggest that γ-Al_2O_3 will form by homogeneous nucleation in isolated liquid droplets of alumina, basically because of its lower liquid-solid interfacial energy. In physical terms the interfacial energy reflects the difference in structure between the crystalline phase and the liquid, and the nucleus would therefore be expected to be the phase with structure most nearly approaching that of the liquid. From this point of view, Plummer's suggestion [1] that the metastable phase observed has a structure closer to that of the liquid would seem correct; however, it is not a matter of "quenching in" of the liquid structure since γ-Al_2O_3 nuclei would form in isolated droplets irrespective of cooling rate.

Das and Fulrath [2] also suggested that the formation of metastable alumina phases in plasma-sprayed material was associated with nucleation kinetics but they did not take into account the possibility of transformation to α-Al_2O_3 after nucleation. Moreover, their approach of considering the effect of cooling rate on the ratio of nucleation rates of two phases will only be applicable if the critical nucleation free energies of the two phases are quite close at T_S.

If γ-Al_2O_3 is nucleated, the factors which determine the phase finally observed are the thermal history of the solid during and after

solidification, and the kinetics of transformations from γ-Al_2O_3 to phases with lower free energies of formation. The temperature-time relationship during the solidification exotherm, which determines whether transformation to α-Al_2O_3 will occur, depends basically upon particle diameter and is relatively insensitive to the overall cooling rate of the gas stream, or possible variations of gas thermal conductivity. This explains the observations that the diameter range over which α-Al_2O_3 occurs in spheroidized particles is very similar for particles spheroidized in flames, d.c. plasma jets and r.f. plasmas. The cooling rate after solidification however will tend to control the transformation from γ-Al_2O_3 to intermediate polymorphs. Thus γ-Al_2O_3 is observed in coatings and small particles spheroidized in a d.c. plasma jet in which rapid cooling rates are achieved, whereas δ-Al_2O_3 and θ-Al_2O_3 are observed in flame and r.f. plasma-spheroidized particles with relatively slow cooling rates after solidification.

Similar considerations as those discussed in this paper could apply to the formation of metastable phases of other materials prepared by high-temperature techniques and it is possible that previously unreported metastable phases could be formed in other systems. In the case of submicron particles of TiO_2 prepared by plasma [41] or flame [42] oxidation of $TiCl_4$ and plasma-spheroidized titania [26, 42], a similar particle-size dependence of constitution is observed, the metastable anatase form generally occurring in small particles and the equilibrium rutile form occurring in large particles. The particle-size range over which rutile becomes the predominant phase is however not clearly defined and appears to be sensitive to the presence of foreign ions [41, 43] an effect which is probably associated with the sensitivity of anatase-rutile transformation to impurities and stoichiometry [44].

Acknowledgements

The work described in this paper was carried out whilst the author was on leave from Monash University, with the Division of Inorganic and Metallic Structure, National Physical Laboratory. Thanks are due to Monash University for providing the opportunity and the National Physical Laboratory for provision of facilities. Helpful discussions with colleagues at NPL are gratefully acknowledged.

References

1. M. PLUMMER, *J. Appl. Chem.* **8** (1958) 35.
2. A. R. DAS and R. M. FULRATH, "5th Int. Symp. Reactivity of Solids", ed. G. M. Schwab (Elsevier, Amsterdam 1965).
3. J. HARVEY, H. I. MATTHEWS, and H. WILMAN, *Discuss Faraday Soc.* **30** (1960) 113.
4. T. I. BARRY, R. K. BAYLISS, and L. E. LAY, *J. Mater. Sci.* **3** (1968) 229.
5. J. P. CUER, J. ELSTON, and S. J. TEICHNER, *Bull. Soc. Chim. France* (1961) 89.
6. N. N. AULT, *J. Amer. Ceram. Soc.* **40** (1957) 69.
7. P. ZOLTOWSKI, *Rev. Int Hautes Tempér et Refract* **5** (1968) 253.
8. J. P. HUFFADINE and A. G. THOMAS, *Powder Met.* **7** (1964) 290.
9. J. P. CUER, J. ELSTON, and S. J. TEICHNER, *Bull. Soc. Chim. Franc.* (1961) 94.
10. D. R. STULL, ed., "JANAF Thermochemical Tables" (Dow Chemical Co, Michigan, 1967).
11. K. A. JACKSON, D. R. UHLMANN, and J. D. HUNT, *J. Crystal Growth* **1** (1967) 1.
12. J. D. HOLMGREN, J. O. GIBSON, and C. SHEER, "Ultrafine Particles", ed. W. E. Kahn (Wiley, New York, 1963).
13. D. TURNBULL, *J. Chem. Phys.* **18** (1950) 768.
14. *Idem, ibid* **20** (1952) 411.
15. E. K. BIGGS, *Proc. Phys. Soc.* **B.66** (1953) 688.
16. D. TURNBULL, *J. Appl. Phys.* **21** (1950) 1022.
17. E. R. BUCKLE, *Discuss Faraday Soc.* **30** (1960) 46.
18. R. E. CECH, *Trans. AIME* **206** (1956) 585.
19. E. R. BUCKLE, *Proc. Roy. Soc.* **A261** (1961) 189.
20. W. G. COURTNEY, *J. Chem. Phys.* **36** (1962) 2009.
21. A. S. SKAPSKI, *Acta Metallurgica* **4** (1956) 576.
22. A. I. KAZNOFF and L. N. GROSSMAN, "Thermodyamics of Nuclear materials" (International Atomic Energy Agency, Vienna 1968), 25.
23. T. YOKOKAWA and O. J. KLEPPA, *J. Phys. Chem.* **68** (1964) 3246.
24. Y. S. TOULOUKIAN ed., "Thermophysical Properties of High Temperature Solid Materials" (MacMillan, New York, 1967).
25. W. D. KINGERY, *J. Amer. Ceram. Soc.* **42** (1959) 6.
26. R. K. BAYLISS, private communication.
27. F. CABANNES, J. CHAPELLE, M. DECROISETTE, and A. SY, *Rev Int. Hautes Temp. et Refract.* **2** (1965) 297.
28. S. A. PANFILOV and YEU. V. TSVETKOV, *Teplofizika Temperatur* **5** (1967) 294.
29. J. W. CAHN, W. B. HILLIG, and G. W. SEARS, *Acta Metallurgica* **12** (1964) 1421.
30. J. D. MCKENZIE, *Adv. Inorg. Rad. Chem.* **4** (1962) 293.
31. A. J. CHAPMAN, "Heat Transfer" (MacMillan, New York, 1967).
32. Y. S. TOULOUKIAN ed., "Thermophysical Properties of Matter" Vol. 3 (Plenum, New York, 1970).
33. B. C. LIPPENS and J. H. DE BOER, *Acta Cryst.* **17** (1964) 1312.

34. A. L. DRAGOO and J. J. DIAMOND, *J. Amer. Ceram. Soc.* **50** (1967) 568.
35. H. SAALFELD and B. MEHROHTA, *Ber. Deutsch. Keram. Ges.* **42** (1965) 161.
36. C. J-P STEINER, D. P. H. HASSELMAN, and R. M. SPRIGGS, *J. Amer. Ceram. Soc.* **54** (1972) 412.
37. R. F. WATERS, J. B. PERI, G. S. JOHN, and H. SEELIG, *Ind. Eng. Chem.* **52** (1960) 45.
38. H. YANAGIDA, G. YAMAGUCHI, and J. KUBOTA, *J. Ceram. Ass. Japan* **74** (1966) 371.
39. W. OSTWALD, *Z. Physik. Chem.* **33** (1897) 289.
40. G. TAMMANN, "The States of Aggregation" (Constable, London, 1926).
41. T. I. BARRY, R. K. BAYLISS, and L. E. LAY, *J. Mater. Sci.* **3** (1968) 239.
42. J. LANG and S. J. TEICHNER, *Rev. Int. Hautes Temp. et Refract.* **2** (1965) 47.
43. R. GERUSZ, P. VERGNON, F. JUILLET, and S. J. TEICHNER, *Comptes Rendus des Journes d'Etude sur les Solides Finement Divisés, Paris* (1969) 233.
44. R. D. SHANNON and J. A. PASK, *J. Amer. Ceram. Soc.* **48** (1965) 391.

Received 15 September and accepted 31 October 1972.